Polymer-Brush Lubricated Surfaces with Colloidal Inclusions under Shear Inversion

L. Spirin,[1,2,3] A. Galuschko,[4,5] T. Kreer,[1,3,4] K. Binder,[1] and J. Baschnagel[4]

[1]*Institute of Physics, Johannes Gutenberg-University, Staudingerweg 7, 55099 Mainz, Germany*
[2]*Graduate School Materials Science in Mainz, Staudingerweg 9, 55128 Mainz, Germany*
[3]*Leibniz Institut für Polymerforschung, Hohe Straße 6, 01069 Dresden, Germany*
[4]*Institut Charles Sadron, 23 rue du Loess, BP 84047, 67034 Strasbourg Cedex 2, France*
[5]*Institut für theoretische Physik, Georg-August Universität, 37077 Göttingen, Germany*

(Received 25 January 2011; published 20 April 2011)

We characterize the response of compressed, sheared polymer-brush bilayers with colloidal inclusions to highly nonstationary inversion processes by means of molecular dynamics simulations and scaling theory. Bilayers with a simple (dimeric) solvent reveal an overshoot for the shear stress, while simulations of dry brushes without explicit solvent molecules fail to display this effect. We demonstrate that mechanical instabilities can be controlled by the inclusion of macromolecular structures, such as colloids of varying softness. Based on a recently developed theory, we suggest a scaling approach to determine a characteristic time for conformational and collective responses.

DOI: 10.1103/PhysRevLett.106.168301 PACS numbers: 47.57.Ng, 83.80.−k, 87.85.gf, 87.85.gp

First experiments [1] on polymer-brush lubricated surfaces date back to the early 1990s. Nowadays, polymer-brush lubrication is a field of large research activity (see, e.g., Refs. [2–7]), which mainly stems from the desire for reducing or controlling the friction forces between surfaces in relative sliding motion. While the observation of extremely small kinetic friction coefficients has stimulated first interesting applications, as, for example, in the design of artificial joints [4], the theoretical understanding is still incomplete. Since most of the investigations have been devoted to (quasi-)stationary processes, as for instance steady or oscillatory shear motion, little is known about nonstationary polymer-brush lubrication. The same applies to polymer-brush lubricated surfaces with embedded macromolecules, as they appear in nature, e.g., in mammalian synovial joints [5].

In this Letter, we report numerical data for conformational and collective quantities of polymer-brush bilayers during a highly nonstationary process, the quasi-instantaneous [8] inversion of the shear direction. Starting from a steady-state configuration, this scenario reflects experiments of large amplitude oscillatory shear (LAOS) [9], where the microscopic structure of the bilayer reaches steady state before the shear direction is inverted.

We compare models for bilayers without explicit solvent, as they have been used widely in the past [10–14], to bilayers with solvent molecules of various structures, from a simple fluid to complex colloidal liquids. For the latter we distinguish between ''hard'' and ''soft'' colloidal inclusions, mimicked as polymer stars of different functionalities and arm lengths. This represents a first step towards the investigation of polymer-brush lubrication with macromolecular inclusions. Our numerical data imply that mechanical instabilities, such as the occurrence of shear forces larger than the steady-state values, can be controlled via concentration and structure of macromolecular inclusions.

Apart from synovial joints, many other biological systems contain brushlike structures and most of them also contain macromolecular inclusions, e.g., capillaries in plants or bloodstream. As we demonstrate below, such inclusions increase the frictional loss within the bilayer, but bear the distinct advantage of stabilizing nonstationary processes. This should be very important for the understanding of biological transport processes.

As in previous studies [13–15], we use the well-established Kremer-Grest polymer model [16], which represents monomers as Lennard-Jones (LJ) spheres connected by the finitely extensible nonlinear elastic potential [16]. Monodisperse polymer chains of $N = 30$ or $N = 60$ repeating units are attached to a flat surface at densities corresponding to slightly more than 2 or 4 times the critical grafting density, from which on the chains start to overlap. Applying good solvent conditions, the chains stretch away from the surface and form a semidilute brush [15].

Compressing two polymer-brush covered surfaces to a bilayer of small thickness ($d = 17.5$ in LJ units), we compare different solvent cases: case A is an implicit solvent (i.e., a solvent-free bilayer), where temperature is kept constant ($T = 1.68$ for all cases) by a dissipative particle dynamics thermostat [17]. The latter reproduces hydrodynamic correlations under steady shear conditions [6,7]. For case B, the bilayer contains dimers mimicked as polymer chains of length $N = 2$ as solvent molecules, with a total (brush and solvent) monomer number density of $\rho = 0.9$. Case $C1$ reflects a complex solvent consisting of dimers and polymer stars with $f = 30$ arms and $m = 5$ monomers per arm, where each arm is connected to one central monomer. While these stars represent hard colloids, soft ''hairy'' colloids are modeled by $f = 10$ and $m = 15$

 © 2011 American Physical Society

(case $C2$). Approximately half of the solvent [18] is exchanged by colloids, keeping $\rho = 0.9$. For case $D1$ ($D2$), we replace virtually all solvent dimers of $C1$ ($C2$) by polymer stars. All particles, the atomically smooth substrates and monomers of brushes, dimers, and stars, are described by the same LJ potential. The below described effects therefore do not depend on chemical details but are of a purely entropic nature.

Figure 1 contains a snapshot of a simulated bilayer with colloidal inclusions ($C1$) at large steady shear. The colloids accumulate in the interface between the brushes, reducing the overlap thickness of the opposing brushes. The amount of overlap determines the response of the bilayer to shear [6,7,13,14]. It can be characterized by the number of binary interbrush contacts per unit time [13,14], N_{int}. While N_{int} decreases with shear rate, we observe a reduced overlap due to the colloidal inclusions at all shear rates including static equilibrium (Fig. 1).

In our simulations, shear inversion takes place at a constant separation between the horizontally aligned, grafted layers. Starting from a well-equilibrated steady-state configuration the substrates' velocities are inverted smoothly, i.e., with a finite acceleration within a time τ_i. To reproduce an instantaneous inversion process, we choose $\tau_i \ll \tau_s$, where τ_s represents the characteristic relaxation time of the bilayer.

Our recently developed scaling theory [6,7] suggests that τ_s is determined by the amount of overlap between the two opposing brushes, yielding

$$\tau_s \sim N^{2.31}(\sigma/d)^{0.31}, \tag{1}$$

with d the distance between the grafted layers, N the length of grafted polymers, and σ their surface (grafting) density. Equation (1) allows for predicting conformational and collective properties of compressed bilayers when they are subject to shear with constant relative velocity v or shear rate $\dot{\gamma} = v/d$ [6,7].

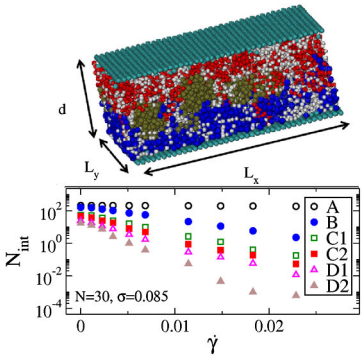

FIG. 1 (color online). Number of binary interbrush contacts per unit time as a function of shear rate. Compared to solvent-free systems (A) and systems with a simple dimeric solvent (B), macromolecular inclusions decrease the overlap between the brushes. Above: Snapshot of a sheared bilayer with colloidal inclusions ($C1$) at large shear.

The conformational response may be characterized by the mean-square radius of gyration of the grafted chains in shear direction, r^2. The upper panel of Fig. 2 shows the ratio between the lateral chain extension at constant shear rate, $r^2(\dot{\gamma})$, and its corresponding value at zero shear, $r^2(0)$. The data are shown as a function of the Weissenberg number, $W \equiv \dot{\gamma}\tau_s$, on a double-logarithmic scaling plot. As predicted by our recent approach [6,7], the structure is independent of W for $W \ll 1$ and $r^2(\dot{\gamma})/r^2(0) \sim W^{0.53}$ in the limit of strong shear ($W \gg 1$), even for the cases $D1$ and $D2$. This implies that the colloidal inclusions relax significantly faster than the grafted chains, which hence dominate the response.

When the bilayer maintains its incompressibility under shear, the kinetic friction coefficient μ scales linearly with W for small shear rates ($W \ll 1$) and as $\mu \sim W^{0.54}$ in the limit far beyond linear response ($W \gg 1$) [6,7]. This behavior can be observed in the lower panel of Fig. 2, where we compare the kinetic friction coefficient as a function of shear rate for the different above cases.

The basic mechanism that leads to shear thinning for polymer-brush coated surfaces is the ability of the grafted chains to stretch in shear direction and decrease the overlap thickness of the bilayer [6,7,13,14]. With colloidal inclusions, the overlap is smaller than for pure brushes (solvents A and B). However, much of the dissipation now occurs between brushes and colloids. Since the colloids themselves can hardly align in shear direction, they lead to larger friction and μ increases with the concentration of the inclusions (from $C1$ to $D1$).

The fact that colloidal inclusions increase the frictional loss within the bilayer (as compared to B, see Fig. 2) might imply the conclusion that, instead of bearing advantages, such molecular structures rather disimprove the lubrication properties. This is indeed the case for steady shear motion. On the other hand, macromolecular inclusions result from a long evolutionary process in nature. Below, we show first evidence of a distinct advantage for nonstationary

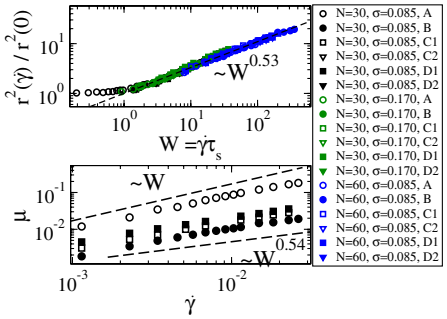

FIG. 2 (color online). Upper panel: Double-logarithmic scaling plot for the chain extension in shear direction. Lower panel: Kinetic friction coefficient as a function of shear rate. While linear response is observed for small shear, both quantities reveal the predicted power laws (see text and Refs. [6,7]) for large shear.

processes, when the colloidal inclusions "smooth" mechanical instabilities during shear inversion. To demonstrate this effect, we compare conformational and collective responses for the above introduced solvent cases.

The main panel of Fig. 3 shows the time evolution of the shear stress [19], $\sigma_{xz}(\dot{\gamma}, t)$, normalized by its value at constant shear rate, $\sigma_{xz}(\dot{\gamma}, 0)$, during instantaneous inversion at time $t = 0$. The data suggest two important conclusions: first, comparison of cases A and B reveals that, in contrast to the observation in steady state (see Fig. 2 and Refs. [6,7]), the response of implicit solvent systems to highly nonstationary shear differs qualitatively from that of systems with explicit solvent dimers. While implicit solvent systems do not exhibit an overshoot [14], we observe a shear stress larger than in steady state for case B [20]. This implies that earlier studies have to be critically revisited, when no explicit solvent molecules were included. Our finding of an overshoot for $\sigma_{xz}(\dot{\gamma}, t)$ is in agreement with experimental observations [2], though these experiments were not performed strictly in the LAOS regime.

A second and more important finding is that colloidal macromolecules smooth the response as they reduce the overshoot. The reason can be understood from the inset of Fig. 3, where we show the number of binary interbrush interactions as a function of rescaled time (see below): the overshoot stems from a short increase of the overlap due to a reorientation of the chains along the new shear direction. Note that there exists an intermediate state, where the grafted chains are directed normal to the substrate; the overlap is hence larger than in steady state and can even exceed its value in static equilibrium (see Fig. 1). Since colloidal inclusions reduce the overlap between the opposing brushes and can by themselves not deform sufficiently to change their overlap with the brushes significantly, they soften the inversion process and reduce or even completely suppress the overshoot. This observation may be important for technical applications as for the understanding of biological systems, where macromolecular inclusions are by far more common than pure polymer-brush bilayers.

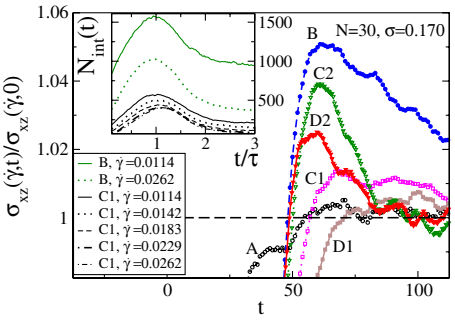

FIG. 3 (color online). Nonstationary shear stress during shear inversion as a function of time. Implicit solvent systems (A) show a smooth crossover to steady state, while the dimeric solvent (B) reveals an overshoot. Macromolecular inclusions reduce this overshoot and for hard colloids of large density ($D1$, see text) it vanishes completely. Inset: Rescaled time development of the number of binary interbrush contacts. The absolute height of the maximum is the largest for systems with dimers and is small for systems that contain inclusions.

The data in the inset of Fig. 3 are presented such that the maxima in $N_{\mathrm{int}}(t)$ align. The scaling is achieved by renormalizing the time axis using a characteristic time τ. We now want to develop an expression for τ in the limit of strong shear. Starting from a steady-state configuration deep in the nonlinear regime ($W \gg 1$), where the chains are strongly stretched laterally [$r(\dot{\gamma}) \sim N$], the shear direction is instantaneously inverted. In this limit, chain relaxation is slow compared to the inversion process and can be neglected on short time scales. The grafting point travels towards the free chain end with a constant velocity $\dot{\gamma}d/2$ reaching it after traveling a distance $r(\dot{\gamma}, \tau)$ and we observe, in agreement with an earlier study [14], a maximum for $N_{\mathrm{int}}(t)$. In the following, we identify the characteristic time from this process. The chain extension develops from the start of the inversion towards the moment of maximal overlap as

$$r(\dot{\gamma}, t)/r(\dot{\gamma}) = 1 - t\dot{\gamma}d/2r(\dot{\gamma}), \tag{2}$$

with $r(\dot{\gamma})$ the steady state and $r(\dot{\gamma}, t)$ the time-dependent lateral chain extension; i.e., we may write

$$\tau \sim r(\dot{\gamma})/\dot{\gamma}d. \tag{3}$$

On the other hand, for $W \gg 1$, we know that $r(\dot{\gamma}) \sim r(0)W^{0.53/2}$ [6,7], thus

$$\tau \sim r(0)\tau_s^{0.27}/\dot{\gamma}^{0.74}d. \tag{4}$$

Using this relation, we obtained the scaling plot in the inset of Fig. 3. To obtain the maximum at $t/\tau = 1$ we introduce a prefactor in Eq. (4) of approximately 100. For the examples presented in Fig. 3, this prefactor does not depend on the system parameters. However, slight deviations are found for the other systems with colloidal inclusions ($C2$,$D1$,$D2$). This is not surprising, as a weak dependence of the monomer mobility is expected for different compositions.

To express τ as a function of the molecular parameters, we use the result of a previous study [6],

$$r(0) \sim N^{0.38}(d/\sigma)^{0.12}. \tag{5}$$

Together with Eqs. (1) and (5) we obtain

$$\tau \sim N/\dot{\gamma}^{0.74}\sigma^{0.04}d^{0.96}, \tag{6}$$

i.e., roughly $\tau \sim N/\dot{\gamma}^{0.74}d$, implying thus a very weak dependence of τ on the grafting density.

The left panel of Fig. 4 shows a successful scaling plot for the time evolution of the shear stress, except for case A. The reason for this failure should be that the steady-state configurations are not far enough in the regime of nonlinear response, as can be seen from Fig. 2. This can also be concluded from the conformational change of the bilayer

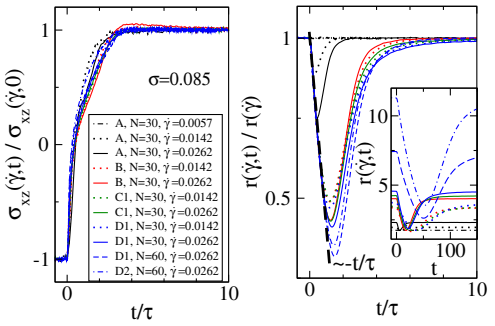

FIG. 4 (color online). Scaling plots for the time development of shear stress (left panel) and chain extension (right panel). Apart from the solvent-free case (A), the data for the shear stress can be brought onto a master curve using the characteristic time [Eq. (4)] (albeit small deviations due to the overshoot). The chain extension follows the predicted behavior before the minimum is reached and the relaxation of the chains sets in. For implicit solvent systems, the maximum is left earlier because the systems are too close to the regime of linear response. Inset: Unscaled data.

during shear inversion. In the right panel of Fig. 4, we show the time evolution of the ratio $r(\dot{\gamma}, t)/r(\dot{\gamma})$ as a function of rescaled time t/τ. The normalized lateral chain extension follows a master curve until a minimum is reached. This happens at a characteristic time, which is proportional to the predicted time scale [Eq. (4)]. However, case A does not follow this trend. Systems with smaller Weissenberg numbers exhibit their minimum earlier and for $W \ll 1$ we find no response of $r(\dot{\gamma}, t)$.

In conclusion, we have demonstrated how the short-time response of conformational and collective quantities of polymer-brush bilayers (with and without inclusions) to a highly nonstationary inversion process can be analyzed in terms of a characteristic time scale. The latter is determined by the increase of overlap between the brushes due to the inversion. We observe no overshoot for the shear stress for solvent-free bilayers, as previously reported [14]. When solvent dimers are included at large density, such that the system is incompressible in steady state, the shear stress can exceed its steady-state value due to an increase of the interbrush interactions shortly after the inversion. Our simulations indicate that it may be possible to stabilize highly nonstationary processes with macromolecular inclusions. This should be of relevance in technical applications and may furthermore explain why nature "uses" such inclusions, for instance to protect biological tissues against rupture. In natural systems, such as joints in animals, innumerous shear inversions occur without any sign of wear and we speculate that, in this context, the lack of shear stress overshoot is favorable.

We thank the Agence Nationale de la Recherche (ANR-06-BLAN-0315), the MENESR, and the "Exzellenzinitiative des Bundes und der Länder" for financial support. T. K. and L. S. thank the European Science Foundation (ESF) for support.

[1] J. Klein, D. Perahia, and S. Warburg, Nature (London) **352**, 143 (1991).
[2] R. Tadmor, J. Janik, J. Klein, and L. J. Fetters, Phys. Rev. Lett. **91**, 115503 (2003).
[3] *Polymer Brushes*, edited by R. C. Advincula, W. J. Brittain, K. C. Caster, and J. Rühe (Wiley-VCH, Weinheim, 2004).
[4] T. Moro, Y. Takatori, K. Ishihara, T. Konno, Y. Takigawa, T. Matsushita, U. Chung, K. Nakamura, and H. Kawaguchi, Nature Mater. **3**, 829 (2004).
[5] J. Klein, Proc. Instn. Mech. Engrs. Part J **220**, 691 (2006); Science **323**, 47 (2009).
[6] A. Galuschko, L. Spirin, T. Kreer, A. Johner, C. Pastorino, J. Wittmer, and J. Baschnagel, Langmuir **26**, 6418 (2010).
[7] L. Spirin, A. Galuschko, T. Kreer, A. Johner, J. Baschnagel, and K. Binder, Eur. Phys. J. E **33**, 307 (2010).
[8] As explained below, we refer to a rapid inversion with finite acceleration.
[9] W. Philippoff, Trans. Soc. Rheol. **10**, 317 (1966).
[10] M. Murat and G. S. Grest, Phys. Rev. Lett. **63**, 1074 (1989).
[11] P. S. Doyle, E. S. G. Shaqfeh, and A. P. Gast, Phys. Rev. Lett. **78**, 1182 (1997); Macromolecules **31**, 5474 (1998).
[12] G. S. Grest, *Advances in Polymer Science*, edited by S. Granick (Springer, Berlin, 1999), Vol. 138, p. 149.
[13] T. Kreer, M. H. Müser, K. Binder, and J. Klein, Langmuir **17**, 7804 (2001).
[14] T. Kreer, K. Binder, and M. H. Müser, Langmuir **19**, 7551 (2003).
[15] T. Kreer, S. Metzger, M. Müller, K. Binder, and J. Baschnagel, J. Chem. Phys. **120**, 4012 (2004).
[16] K. Kremer, G. S. Grest, and I. Carmesin, Phys. Rev. Lett. **61**, 566 (1988).
[17] P. J. Hoogerbrugge and J. M. V. A. Koelman, Europhys. Lett. **19**, 155 (1992); P. Espanol and P. Warren, Europhys. Lett. **30**, 191 (1995).
[18] The ratio of solvent and colloid monomer densities depends on the molecular parameters of brushes and colloids and cannot be adjusted precisely to 1.
[19] We calculate the shear stress using the Irving-Kirkwood method; J. H. Irving and J. G. Kirkwood, J. Chem. Phys. **18**, 817 (1950).
[20] Similar conclusions can be drawn from the normal stress (not shown).